NeuroImage: Clinical 32 (2021) 102809

Contents lists available at ScienceDirect

NeuroImage: Clinical

journal homepage: www.elsevier.com/locate/ynicl

A quantitative analysis of the retinofugal projections in congenital and late-onset blindness

Maurice Ptito [a,b,c], Samuel Paré [a], Laurence Dricot [d], Carlo Cavaliere [e,f], Francesco Tomaiuolo [g], Ron Kupers [a,b,d,*]

[a] School of Optometry, University of Montreal, Montreal, QC, Canada
[b] BRAINlab, University of Copenhagen, Copenhagen, Denmark
[c] Danish Research Center for Magnetic Resonance (DRCMR), Copenhagen University Hospital, Hvidovre, Denmark
[d] Institute of NeuroScience (IoNS), Université catholique de Louvain (UCLouvain), Belgium
[e] IRCCS SDN, Naples, Italy
[f] Coma Science Group, Cyclotron Research Center and Neurology Department, University and University Hospital of Liège, Liège, Belgium
[g] Univesità degli Studi di Messina, Dipartimento di Medicina Clinica e Sperimentale

ARTICLE INFO

Keywords:
Vision
Blindness
Plasticity
White matter
Optic chiasm
Lateral geniculate nucleus

ABSTRACT

Vision loss early in life has dramatic consequences on the organization of the visual system and hence on structural plasticity of its remnant components. Most of the studies on the anatomical changes in the brain following visual deprivation have focused on the re-organization of the visual cortex and its afferent and efferent projections. In this study, we performed a quantitative analysis of the volume and size of the optic chiasm, optic nerve, optic tract and the lateral geniculate nucleus (LGN), the retino recipient thalamic nucleus. Analysis was carried out on structural T1-weighted MRIs from 22 congenitally blind (CB), 14 late blind (LB) and 29 age -and sex-matched sighted control (SC) subjects. We manually segmented the optic nerve, optic chiasm and optic tract, while LGN volumes were extracted using in-house software. We also measured voxel intensity of optic nerve, optic chiasm and optic tract. Mean volumes of the optic nerve, optic tract and optic chiasm were reduced by 50 to 60% in both CB and LB participants. No significant differences were found between the congenitally and late-onset blind participants for any of the measures. Our data further revealed reduced white matter voxel intensities in optic nerve, optic chiasm and optic tract in blind compared to sighted participants, suggesting decreased myelin content in the atrophied white matter. The LGN was reduced by 50% and 44% in CB and LB, respectively. In LB, optic nerve volume correlated negatively with the blindness duration index; no such correlation was found for optic chiasm, optic tract and LGN. The observation that despite the absence of visual input about half of the subcortical retinofugal projections are structurally preserved raises the question of their functional role. One possibility is that the surviving fibers play a role in the maintenance of circadian rhythms in the blind through the intrinsically photosensitive melanopsin-containing retinal ganglion cells.

1. Introduction

The organization of the visual system in mammals is such that the information entering the eye is processed through the retinal mosaic to reach the retinal ganglion cells whose axons form the optic nerve. Half the ganglion cell axons decussate at the level of the optic chiasm to reach the lateral geniculate nucleus (LGN) of the thalamus that projects to the primary visual cortex (Krug, 2012). Consequently, damage to the retina will have considerable impact on the anatomo-functional organization of the retinofugal system. A multitude of animal studies on various forms of early life visual deprivation (enucleation, eyelid suturing, dark rearing) have highlighted the alterations not only in white matter projections but also in thalamic and cortical grey matter retino-recipient structures (Chabot et al., 2008; Desgent and Ptito, 2012; Hoffmann and Dumoulin, 2015). In humans, pathologies of the eyes such as glaucoma, strabismus, albinism and enucleation also lead to major changes of the retinofugal pathways, including a reduction and alteration in the configuration of the optic chiasm (Hoffmann and Dumoulin, 2015;

* Corresponding author at: Department of Neuroscience & Pharmacology, Faculty of Health & Medical Sciences – Panum Institute, University of Copenhagen, Blegdamsvej 3B, 2200 Copenhagen, Denmark.
E-mail address: kupers@sund.ku.dk (R. Kupers).

https://doi.org/10.1016/j.nicl.2021.102809
Received 23 March 2021; Received in revised form 14 July 2021; Accepted 24 August 2021
Available online 27 August 2021

Schmitz et al., 2003) and degeneration of the optic tracts and LGN (Beatty et al., 1982; Hickey and Guillery, 1979; Schmitz et al., 2003; You et al., 2012). In the case of retinoblastoma, early monocular enucleation affects several parts of the retinofugal projections such as reduced contralateral optic nerve and ipsi- and contralateral optic tract diameters, optic chiasm volume and width, and reduced volume of the ipsilateral LGN (Kelly et al., 2013). In congenital blindness (CB) resulting from various eye pathologies (e.g. retinopathy of prematurity, Leber's amaurosis), similar morphological changes to those reported by Kelly et al., (2013) have been described (Breitenseher et al., 1998; Noppeney, 2007; Ptito et al., 2008; Shimony et al., 2006). Interestingly, there exists a large variability in the clinical appearance of the optic chiasm in CB, with some subjects showing a complete atrophy, whereas others have a seemingly normal chiasm (Ptito et al., 2008). Moreover, the primary visual system, including the LGN and visual cortical areas V1 to V5, also shows significant volume reductions (Cecchetti et al., 2016; Noppeney, 2007; Pan et al., 2007; Ptito et al., 2008). In contrast, the superior colliculus remains preserved in CB (Cecchetti et al., 2016) although its thalamic recipient structure, the posterior pulvinar, is reduced in volume (Ptito et al., 2008). Functional and structural connectivity between early visual cortex and higher visual cortex and non-visual cortical areas is also altered (Bedny et al., 2011; Butt et al., 2013; Fortin et al., 2008; Heine et al., 2015; Jiang et al., 2009; Liu et al., 2007; Reislev et al., 2016b; Reislev et al., 2017; Wang et al., 2013; Watkins et al., 2013). Finally, the posterior portion of the corpus callosum, linking left and right visual cortical areas, is reduced in volume in both CB and LB (Cavaliere et al., 2020; Ptito et al., 2008; Tomaiuolo et al., 2014), suggesting alterations in interhemispheric connectivity.

Most of the anatomical studies in CB have mainly focused on the structural and functional changes that take place at the cortical level (reviewed in Kupers and Ptito, 2014a). The retinofugal system has received little attention. Although the few available studies concur that there is atrophy of all components of the retinofugal system, the magnitude of the changes has not been quantified. Also, most studies have a limited sample size and have focused nearly exclusively on CB. The aim of this study was therefore to quantify volumetric changes of the optic nerve, optic chiasm, optic tract and LGN in a large sample of CB and LB subjects, using state-of-the-art analysis applied to high-resolution MRI images.

2. Methods

2.1. Subjects

A total of 36 blind, among whom 22 CB and 14 LB, and 29 normal sighted controls (SC) participated in this study. Table 1 displays the demographic characteristics of the blind participants. Mean age of CB, LB and SC was 41.09 ± 13.3 years (range: 20–63), 52.9 ± 15.1 years (range: 25–78 and 39.8 ± 12.9 (range: 22–61), respectively. The ratio of male (M) to female (F) participants was 13 M/9F for CB, 7 M/7F for LB and 16 M/13F for SC. Mean blindness onset age in the LB group was 17.1 ± 13.3 years (range: 2–50), mean blindness duration was 35.9 ± 14.0 years (range: 6–60) and mean blindness duration index was 0.67 ± 0.24 (range: 0.23–0.95). The blindness duration index was calculated as follows: (*age – age at onset of blindness*) / *age* (Meaidi et al., 2014). The resulting score can vary from 0 to 1, expressing the relative amount of time an individual has been blind, with low scores indicating recent onset of blindness and high scores long duration of blindness. Inclusion criteria were a clinical diagnosis of blindness for blind subjects and normal or corrected normal vision for SC. Exclusion criteria were significant neuro-psychiatric comorbidity and alcohol or drug addiction. All participants had previously been enrolled in other functional or structural brain imaging studies conducted by our group, in which a T1-weighted structural MRI brain scan had been collected. The total sample comes from a Danish (BRAINlab, Copenhagen) and a Canadian (Institut Nazareth et Louis Braille, Montreal) study cohort; they are further

Table 1
Demographic characteristics of the blind participants. BDI, blindness duration index; CB, congenitally blind; CPH, Copenhagen; F, female; LB, late blind; M, male; MTL, Montreal.

Participants	Cohort	Sex	Age	Cause of blindness	Blindness onset (years)	BDI
LB01	CPH	F	36	Glaucoma	8	0.78
LB02	CPH	F	59	Iris infection, cataract	23	0.61
LB03	CPH	M	64	Retinitis pigmentosa	15	0.77
LB04	CPH	M	44	Retinoschisis	9	0.80
LB05	CPH	F	44	Retinal detachment	7	0.84
LB06	CPH	M	78	Retinal detachment	50	0.36
LB07	CPH	F	51	Retinal detachment	32	0.37
LB08	CPH	F	25	Glaucoma, cataract, retinal detachment	19	0.24
LB09	CPH	M	43	Retinoblastoma	2	0.95
LB10	CPH	F	40	Retinoblastoma	2	0.95
LB11	CPH	M	74	Eye trauma	14	0.81
LB12	CPH	M	57	Glaucoma, cataract, retinal detachment	17	0.70
LB13	CPH	F	60	Retinal detachment	31	0.48
LB14	CPH	M	66	Glaucoma	10	0.85
CB01	CPH	M	50	Retinopathy of prematurity	Perinatal	–
CB02	CPH	F	37	Retinopathy of prematurity	Perinatal	–
CB03	CPH	M	59	Retinopathy of prematurity	Perinatal	–
CB04	CPH	F	63	Retinopathy of prematurity, glaucoma	Perinatal	–
CB05	CPH	M	37	Unknown	Perinatal	–
CB06	CPH	M	44	Retinoblastoma	Perinatal	–
CB07	CPH	M	51	Retinopathy of prematurity	Perinatal	–
CB08	CPH	F	29	Retinopathy of prematurity	Perinatal	–
CB09	CPH	M	59	Retinopathy of prematurity	Perinatal	–
CB10	CPH	F	25	Retinopathy of prematurity	Perinatal	–
CB11	CPH	M	27	Retinopathy of prematurity	Perinatal	–
CB12	CPH	F	55	Unknown	Perinatal	–
CB13	CPH	F	28	Retinopathy of prematurity	Perinatal	–
CB14	CPH	F	25	Retinopathy of prematurity	Perinatal	–
CB15	MTL	F	49	Retinopathy of prematurity	Perinatal	–
CB16	MTL	M	41	Retinitis pigmentosa	Perinatal	–
CB17	MTL	M	39	Retinal detachment	Perinatal	–
CB18	MTL	M	58	Congenital cataract	Perinatal	–
CB19	MTL	M	38	Retinopathy of prematurity	Perinatal	–
CB20	MTL	F	31	Glaucoma, aniridia	Perinatal	–
CB21	MTL	M	20	Leber's amaurosis	Perinatal	–
CB22	MTL	M	23	Congenital cataract	Perinatal	–

referred to as the "Copenhagen" and "Montreal" data-sets. The Copenhagen data set was acquired at the Danish Research Center for Magnetic Resonance (DRCMR). The study protocols had been approved by the local research ethics committees and all participants had given their written informed consent.

2.2. MRI scans

The scanning parameters differed slightly for the two study cohorts. For the Canadian volunteers, 3D-MPRAGE structural images of the brain were collected on a 1.5 T Siemens Magnetom Avanto scanner. Sequence parameters were TR = 2240 ms, TE = 9.2 ms, FA = 10°, FOV = 256 × 256 mm, acquisition matrix = 256 × 256, in-plane resolution = 1.91 mm, slice thickness = 1 mm). For the Copenhagen cohort, structural scans were acquired on a 3 T Siemens Verio scanner with a 32-channel head coil using a 3D T1-weighted MPRAGE sequence (TR = 1900 ms, TE = 2.32 ms, FA = 9°, isotropic 0.93 mm^3 voxels).

2.3. Image processing

Scans were converted from DICOM into mgz or nifti format, depending on the brain imaging center where they had been acquired, and then into MINC format (Montreal Neurological Institute, McGill University) that we used for further image processing. In order to standardize the images and correct for interindividual differences in gross brain size, MRI volumes were transformed into MNI space by using "ICBM152" model atlas "bestlinreg.pl" algorithm in MINC (https://github.com/BIC-MNI/EZminc/blob/master/scripts/bestlinreg.pl). For the manual labelling of the optic nerve, optic chiasm and optic tract, the experimenter was unaware to which group the images belonged.

2.4. Retiofugal projections segmentation

We used DISPLAY (http://www.bic.mni.mcgill.ca/software/Display/Display.html), an interactive program developed by the brain imaging center of the Montreal Neurological Institute, to display the optic nerve, optic chiasm, and optic tract. This program permits labelling of voxel regions on each slice of the MRI volume and allows for the simultaneous visualization of the movement of the cursor on the screen within the sagittal, horizontal and coronal planes of the MRI. A selection of any area can be made by using the DISPLAY 'mouse-brush' that marks the voxels by colouring. This colouring procedure accompanied by the simultaneous 3-D view of the MRI planes allows a better identification and selection of the regions of interest. The optic nerve and optic tract were mapped as the structures in continuation of the body of the optic chiasm for four mm to the frontal border and to four mm to the posterior to the occipital border, respectively. After initial segmentation of the optic chiasms, optic nerves and optic tracts, all results were revised to correct for intra-observer variability, if needed. The above method resulted in three-dimensional volumes of the whole optic chiasm and of 4 mm length segments of the optic nerve and optic tract as illustrated in Fig. 1 on a 3D-rendered MRI image.

LGN volumes were extracted in an automated manner using in-house methods and software described in Cecchetti et al., (2016). In brief, we adopted a ROI-based approach that combines an automatic segmentation method (Hernowo et al., 2011) with probabilistic maps registered to the MNI space (Eickhoff et al., 2005; Burgel et al., 2006). The LGN was identified by partitioning the T1 brain image into six tissue classes (instead of the classical three classes of grey mater, white matter and CSF) whereby the fifth tissue class accounts well for the boundary definition of the LGN and medial geniculate nuclei (Hernowo et al. 2011).

2.5. Voxel intensity measurements

The voxel intensity (VI) value is an indirect measure of the myelin content of the axons in that, the higher the myelin content, the higher is the VI signal and vice-versa (Bottomley et al., 1984). The intensity measurements were averaged for every voxel segmented. The data were extracted using the "intensity_statistics" algorithm in MINC (http://www.bic.mni.mcgill.ca/~stever/software_map.html). To take into account the fact that averaged intensity values differed between scans, data were analyzed as a ratio taking the genu of the corpus

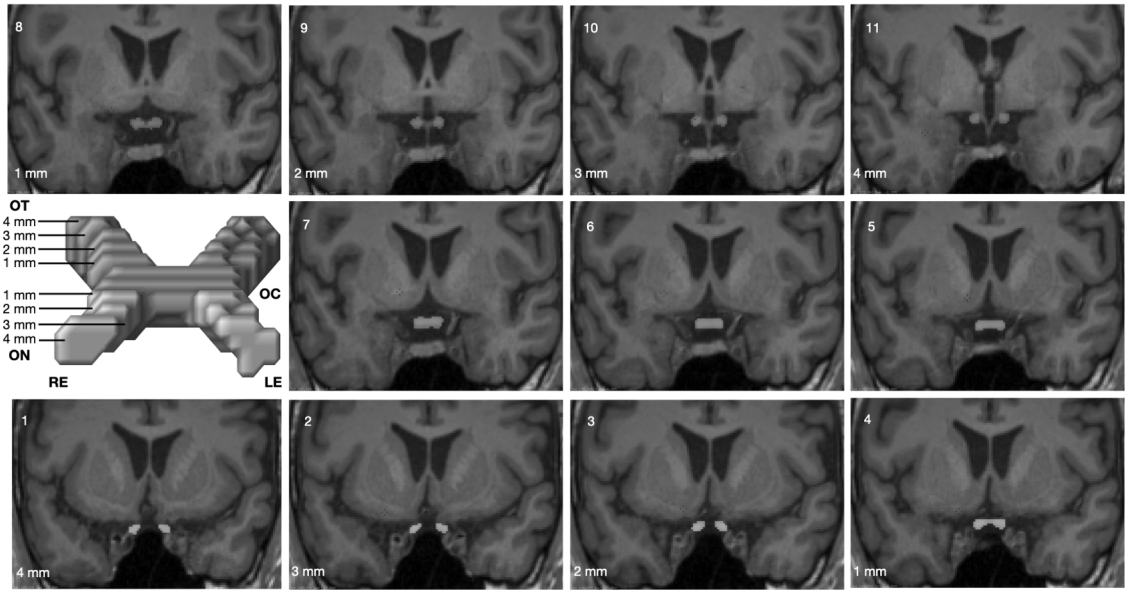

Fig. 1. Anatomical delineation of the optic chiasm. A 3D rendered image of the optic nerve (in yellow), optic chiasm (in green) and optic tract (in cyan) from a sighted participant. We delineated the optic nerve on coronal slices from 4 mm anterior to the frontal border of the optic chiasm body; the optic tract was segmented from 4 mm posterior to the occipital border of the optic chiasm body. The 11 slices are presented in a sequential manner: optic nerve (slices 1–4), optic chiasm (slices 5–7) and optic tract (slices 8–11). Abbreviations: LE, left eye; OC, optic chiasm; ON, optic nerve; OT, optic tract; RE, right eye. (For interpretation of the references to colour in this figure legend, the reader is referred to the web version of this article.)

callosum as white matter reference (e.g. averaged VIs of the chiasm / averaged VIs of the genu), as described in (Tomaiuolo et al., 2002).

2.6. Statistical analysis

The statistical analysis was performed in Jasp, an open-source graphical program for statistical analysis developed by the University of Amsterdam. Two-way ANCOVAs were carried out for all group comparisons with Bonferroni post-hoc tests for multiple comparisons if the ANCOVA signaled significant differences. Where non-Gaussian distributions of outcome variables (optic nerve, optic chiasm, optic tract and VI ratio) were assumed, we used a Kruskall-Wallis test. In case of null findings, in particular between CB and LB groups, we used a Bayesian approach to test whether the negative findings could be explained by a lack of statistical power. Thereto, we calculated the Bayes Factor (BF_{10}) value and compared it to the best model to evaluate if null-findings were driven by a lack of power. We set a $BF_{10} < 1$ as strong evidence in support of the null hypothesis, while a $BF_{10} > 10$ was used as strong evidence for the alternative hypothesis (Lee and Wagenmakers, 2014; Kelter, 2020; Keysers et al., 2020). First, intergroup comparisons were conducted to test for differences between the Copenhagen data and Montreal data-sets. Then, Mann-Whitney t-tests were performed comparing outcome variables for each categorical demographic variable grouping (gender and handedness). The effect of age on outcome variables was then evaluated both with simple linear regressions and with multiple linear regressions including all disease-related independent variables. Finally, the age-corrected effects of all disease-related characteristics (vision yes/no, blindness group, blindness onset age, retinopathy of prematurity versus other causes, years blind, blindness duration index) on outcome variables were analysed separately with multiple linear regressions. We set a *p* value of 0.05 as threshold level for statistical significance. Data are presented as mean ± SD.

3. Results

Intergroup comparisons between the Copenhagen data and Montreal data-sets did not reveal any significant differences between both cohorts. The data of both samples were therefore pooled together. Although age did not have a significant effect in any linear model, we included it in all multivariate analyses since LB participants were older than CB and SC.

3.1. Optic nerve volume

The optic nerve volume was strongly reduced in both CB and LB ($F(2,59) = 121.167$, $p < 0.001$). The mean optic nerve volume in SC was $203.8 \pm 28.2\ mm^3$ compared to $97.5 \pm 20.5\ mm^3$ in CB ($t(49) = -14.111$, $p < 0.001$) and $101.2 \pm 28.5\ mm^3$ in LB ($t(41) = -11.129$, $p < 0.001$), a reduction by 52% and 50%, respectively (Fig. 2, upper part). The optic nerve volume in CB and LB did not differ ($t(34) = -0.486$, $p > 0.05$; $BF_{10} = 0.339$), indicating that onset and duration of blindness have similar effects on optic nerve atrophy.

3.2. Optic chiasm volume

As shown in Fig. 2, ANCOVA revealed a significant group effect for optic chiasm volumes ($F(2,59) = 71.457$, $p < 0.001$). Indeed, the optic chiasm of CB ($99.6 \pm 37.3\ mm^3$; $t(49) = -10.808$, $p < 0.001$) and LB ($111.6 \pm 28.2\ mm^3$; $t(41) = -10.808$, $p < 0.001$)) participants were significantly smaller than that of their sighted counterparts ($210.8 \pm 41.3\ mm^3$). There was no significant difference in mean optic chiasm volume between CB and LB ($t(34) = -0.307$, $p > 0.05$; $BF_{10} = 0.488$). The optic chiasm volume was reduced by 53% and 47% in CB and LB, respectively.

3.3. Optic tract volume

There was a significant effect of group on optic tract volume ($F(2,59) = 182.963$, $p < 0.001$). Mean volume of the optic tract was smaller in CB ($74.6 \pm 26.9\ mm^3$; $t(49) = -17.403 p < 0.001$) and LB ($80.5 \pm 21.9\ mm^3$; $t(41) = -13.571$, $p < 0.001$) when compared to SC ($203.3 \pm 27.4\ mm^3$) (Fig. 2, lower part). This implies a volumetric reduction of the optic chiasm of 64% in CB and 61% in LB, compared to SC. The optic tract volume in CB and LB did not differ ($t(34) = -0.747$, $p > 0.05$; $BF_{10} = 0.409$).

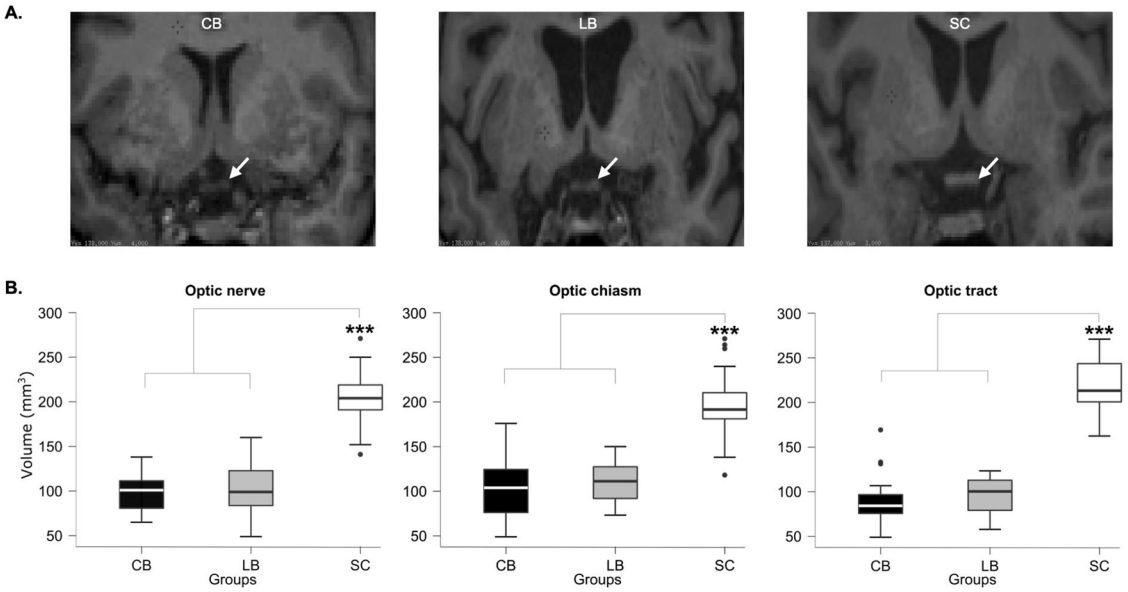

Fig. 2. MRI of the optic chiasm and volumetric measures of the retinofugal projections. A. Examples of the optic chiasm (arrows) in an individual CB, LB and SC participant, shown optic nerve T1 coronal sections. The different size of the optic chiasm between blind and sighted participants is evident by visual inspection. B. Average volumes of optic nerve, optic chiasm and optic tract. The box and whisker plots illustrate the first (bottom box) and third quartiles (top box) of every group separated by their respective median. Distant dots represent outliers. Significant differences are indicated by asterisks (*** = $p < 0.001$). Abbreviations: CB, congenitally blind; LB, late blind; SC, sighted controls.

3.4. Lateral geniculate nucleus volume

Both CB and LB participants had smaller LGN than SCs ($p < 0.001$; Fig. 3A). Average LGN volumes were $52.1 \pm 10.3\ mm^3$, $58.6 \pm 18.9\ mm^3$ and $104.4 \pm 24.8\ mm^3$ for CB, LB and SC, respectively. This corresponds to a volumetric reduction of 50% in CBs ($p < 0.001$) and 44% in LBs ($p < 0.001$) compared to SCs. No significant difference was found between CB and LB groups ($p = 0.951$; $BF_{10} = 0.494$). Age at blindness onset did not have a significant effect on LGN volumes in univariate linear regression analysis of subject groups, or when included in multiple linear regression models. LGN volume did not correlate with age of blindness onset ($r_s = 0.006$, $p = 0.968$) or with blindness duration index scores in LB ($r_s = -0.143$, $p = 0.625$). There was also no significant difference between the left and right LGN size for any groups ($p > 0.05$).

To evaluate the correlation between white matter and LGN volumes, Spearman's rho tests were used since the data had a non-normal distribution. The analyses revealed a positive correlation between optic chiasm volumes and average LGN volumes in SC ($r_s = 0.476$, $p = 0.034$) but not in CB ($r_s = -0.135$, $p = 0.580$) nor LB ($r_s = 0.160$, $p = 0.584$) (Fig. 3B).

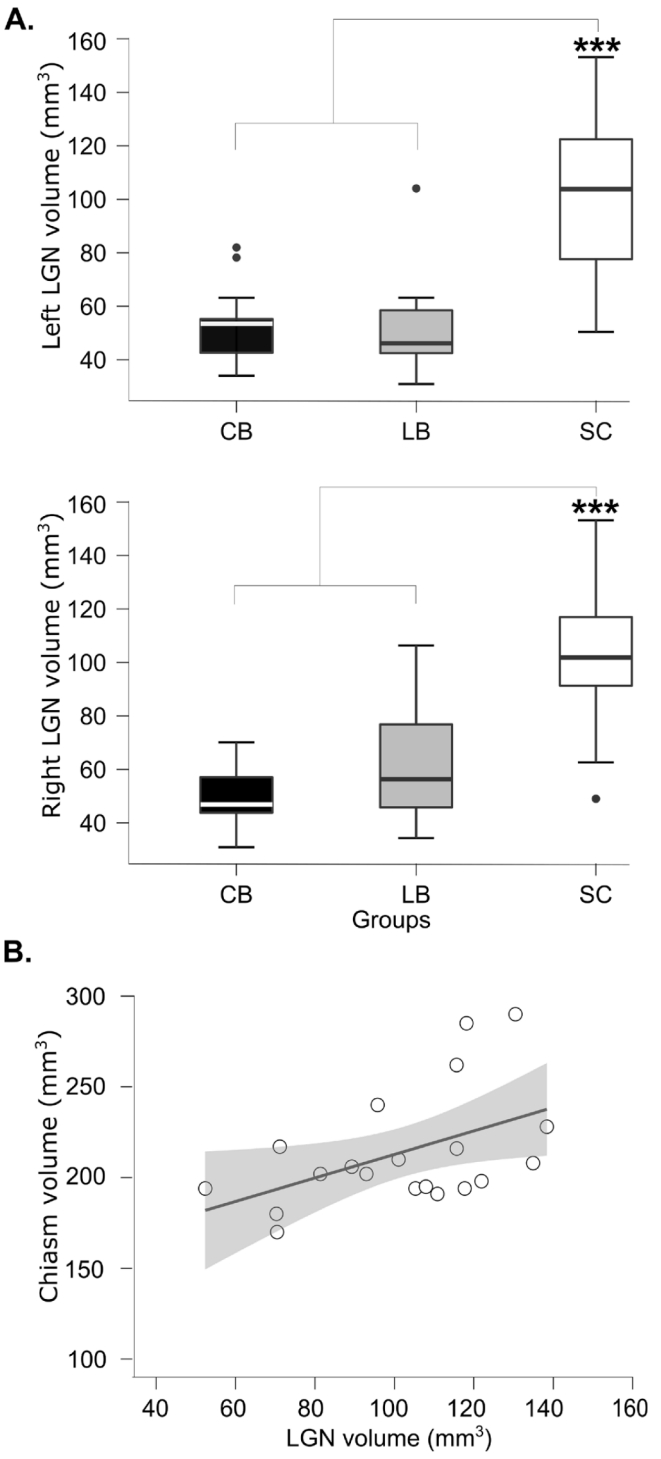

Fig. 3. LGN volumes and correlation with optic chiasm. A. Average volumes of left and right LGN. Significant differences are indicated by asterisks (*** = $p < 0.001$). B. Positive correlation between optic chiasm and average LGN volumetric measures in SC. The grey shading indicates the 95% confidence interval. Abbreviations as in Fig. 2.

3.5. Voxel intensity ratio

Since no significant differences between the optic nerve, the optic chiasm and the optic tract were found for the voxel intensity ratios, they were pooled together and the average ratio of the three structures was

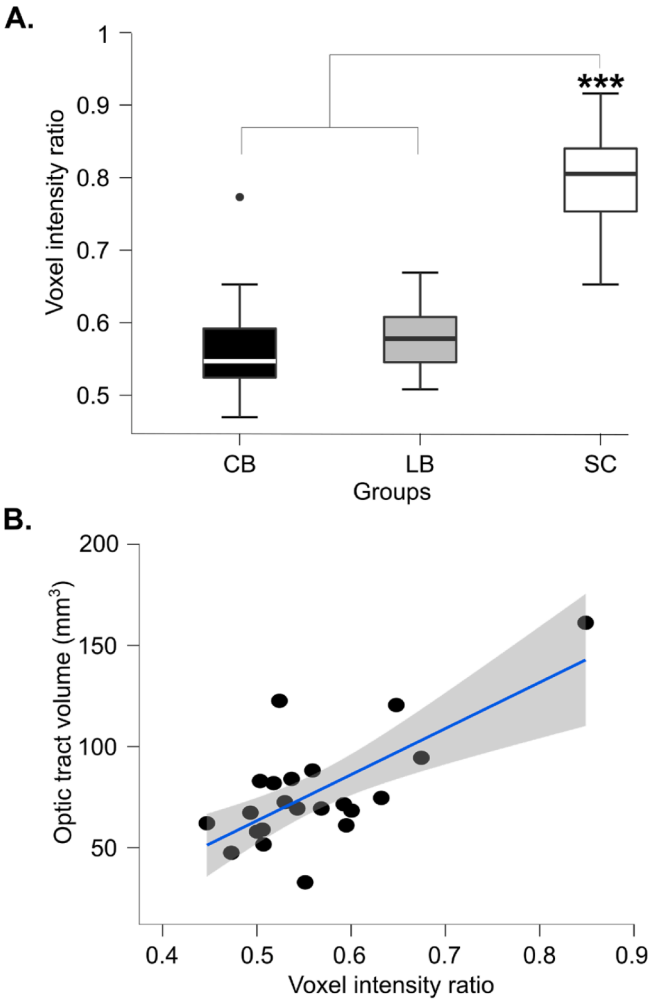

Fig. 4. Voxel intensity ratios and correlation with optic tract volume. A. Voxel intensity ratios for optic nerve, optic chiasm and optic tract combined in the three groups. Significant differences are indicated by asterisks (*** = $p < 0.001$). B. Positive correlation between voxel intensity ratios and volume of the optic tract in CB. The correlation was not uniquely driven by the results from the participant with the most outlying data (right-most data point), since removing this data point from the analysis still yielded a significant correlation ($rs = 0.437$, $p = 0.048$). The grey shading indicates the 95% confidence interval. Abbreviations as in Fig. 2.

used for the analysis. ANCOVA revealed a significant effect of group ($F(2,59) = 97.971$, $p < 0.001$). As shown in Fig. 4A, the voxel intensity ratio was significantly lower in both CB (0.563 ± 0.068; $t(49) = -7.870$, $p < 0.001$) and LB (0.576 ± 0.047; $t(41) = -5.608$, $p < 0.001$) compared to their SC counterparts (0.790 ± 0.064).

To investigate whether white matter volume correlated with voxel intensity ratio, we carried out Spearman's rho tests due to the non-Gaussian distribution of the data. As shown in Fig. 4B, optic tract volumes correlated with voxel intensity ratio for CB ($r_s = 0.511$, $p < 0.05$) but not for LB ($r_s = 0.468$, $p = 0.094$) nor SC ($r_s = 0.082$, $p = 0.674$). No significant correlations were found between voxel intensity ratio and white matter volume of optic nerve and optic chiasm for any of the groups.

3.6. Blindness duration index

As shown in Fig. 5, there was a significant negative correlation between blindness duration index and optic nerve volume in LB ($r_s = -0.591$, $p = 0.026$). However, blindness duration index did not correlate with volume of optic chiasm ($r_s = -0.421$, $p = 0.134$) or optic tract ($r_s = -0.267$, $p = 0.357$). Blindness duration index measures also did not correlate with voxel intensity ratios for any of the three groups.

4. Discussion

The optic chiasm and LGN relay all visual information coming from the retina via the optic nerve. Consequently, lack of visual input at the level of the retina, as in the case of blindness of peripheral origin, is likely to have a major impact on the structural integrity of the retinofugal projections. Although several studies have looked at changes in white matter structure and function in the blind brain, structural changes in the optic chiasm have not been measured quantitatively (Breitenseher et al., 1998; Noppeney, 2007; Pan et al., 2007; Ptito et al., 2008; Shimony et al., 2006). In this study, we examined the structural changes in all subcortical components of the retinofugal projection system of a large group of congenitally and late blind individuals. We manually segmented the optic nerve, chiasm and tracts, and used in-house software to automatically segment the LGN on T1-weighted MRI-scans to obtain quantitative measures of volume and voxel intensity ratio. The present data reveal significant atrophy of the retinofugal components in both congenital and late-onset blindness. All three components, optic nerve, optic chiasm and optic tract were on average less than half the size in blind compared to sighted participants, whereas the LGN was slightly more than half the size of that in sighted controls. Our LGN volumes obtained in normal sighted controls are similar to those obtained in post-mortem brain analyses (Andrews et al., 1997), adding proof to the validity of the automatic segmentation procedure used (Cecchetti et al., 2016). In addition to the volumetric changes, voxel intensity ratio was significantly reduced in all measured areas in CB and LB. Since voxel intensity gives an indirect measure of the myelin content of the axons, our findings suggest a significant loss of myelin in the retinofugal projections in the blind brain. Future studies, providing more direct measures of myelination such as simultaneous tissue relaxometry, magnetization transfer saturation index, and T1w/T2w ratio methods (Hagiwara et al., 2018) should test this hypothesis more directly.

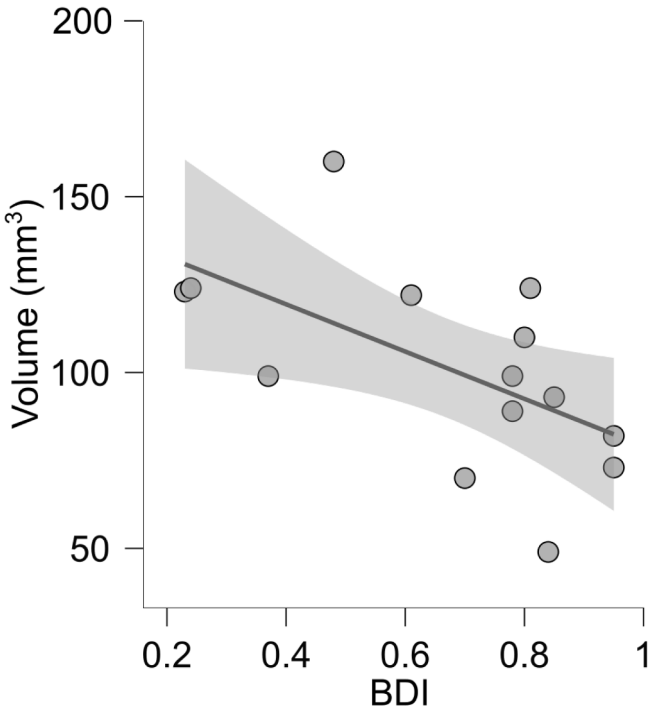

Fig. 5. Correlation between the blindness duration index (BDI) and volume of the optic nerve in LB. BDI correlated negatively with optic nerve volume in LB. The grey shading indicates the 95% confidence interval.

We reported before that the LGN is reduced in volume by around 40% in CB (Cecchetti et al., 2016). Here, we replicate these findings and extend these to late blind subjects. It is interesting to compare the present results of LGN changes with those reported in other conditions affecting the retina, but in which vision is only partically affected. Studies in patients with open angle glaucoma have shown LGN reductions between 25 and 30% (Gupta et al., 2009; Kosior-Jarecka et al., 2020; Lee et al., 2014; Schmidt et al., 2018). Reductions in LGN volume did not correlate with visual field indices (Kosior-Jarecka et al., 2020) but with thickness of the ganglion cell layer and inner plexus layer of the contralateral eye (Lee et al., 2014). A study on albinism showed reductions of between 20 and 30% for optic nerve, optic tract and optic chiasm and of 38% for the LGN which were attributed to a reduction of the retinal ganglion cells in the central retina (Mcketton et al., 2014). Finally, a study in patients suffering from multiple sclerosis reported a 14% reduction in LGN volume that correlated with the thickness of the ganglion cell-inner plexiform layer (Papadopoulou et al., 2019).

4.1. Lack of difference between CB and LB

A rather surprising result was the absence of difference in any of the size measures between congenitally and late blind participants. A possible explanation for this finding might be that all LB participants were blind for at least 6 years. Probably, the atrophic changes take place in the first year(s) after onset of blindness, whereafter the white matter stabilizes without undergoing further atrophic changes. In this respect, a study on the effects of early enucleation in mice showed that the LGN is already reduced by >30% a few days post-enucleation (Kozanian et al., 2015). A recent diffusion imaging study by our group showed similar reduced fractional anisotropy in the ventral stream of CB and LB subjects, regardless of their time of blindness onset (Reislev et al., 2016a). Future studies including LB subjects in the early phase after onset of blindness may shed further light on this issue.

4.2. Significance of the results

The atrophy of the retinofugal projections and LGN in the blind may be due to the degeneration of retinal ganglion cells following various forms of eye pathology. The above finding extend previous reports that pathology to the eyes is associated with atrophy of the optic nerve, tract and chiasm (Breitenseher et al., 1998; Noppeney, 2007; Pan et al., 2007; Ptito et al., 2008), optic radiations (Shimony et al., 2006; Pan et al., 2007; Ptito et al., 2008), LGN (Cecchetti et al., 2016; Kosior-Jarecka et al., 2020; Lee et al., 2014; Schmidt et al., 2018), inferior and superior longitudinal fasciculi (Reislev et al., 2016a), splenium of the corpus

callosum (Ptito et al., 2008; Tomaiuolo et al., 2014, Cavaliere et al., 2020), and the anterior commisure (Cavaliere et al., 2020). Our study therefore supports a body of evidence indicating that subcortical visual pathways atrophy in case of pathology to the retinal ganglion cells. The partial preservation of the retinofugal projections as well as of its retino-recipient thalamic nucleus may suggest that the retina of blind individuals might still contain functional retinal ganglions cells.

Studies in both animals and humans have shown that several types of lesions to the retina (retinal diseases, visual deprivation, enucleation, anophthtalmia) are associated with anatomical changes along the retino-geniculo-striate and collicular pathways. Despite the fact that some of these conditions lead to a complete loss of (image-forming) vision, the atrophy of the chiasm and the LGN is only partial; between 50% and 70% of the LGN remains preserved (Abbott et al., 2015; Cecchetti et al., 2016; Karlen et al., 2006; Kozanian et al., 2015). The most prevalent hypothesis explaining the preservation of a residual visual system is that non-visual (tactile and or auditory) sensory input is funnelled to the LGN and from there to the occipital cortex (Charbonneau et al., 2012; Karlen et al., 2006; Müller et al., 2019).

Studies in patients with Leber's hereditary optic neuropathy (LHON), cone-rod dystrophy and primary open angle glaucoma, have shown decreased fractional anisotropy in the optic chiasm, optic tracts, optic radiations and in the white matter adjacent to the lateral occipital cortex (Bridge et al., 2011; Frezzotti et al., 2014; Manara et al., 2015; Ogawa et al., 2014). Interestingly, Rizzo and co-workers (2012) performed a classical neuropathological examination on post-mortem tissue from a 75 year-old female patient suffering from LHON and a 75 year-old control. The results showed a 42% decrease of neuron soma size in the magnocellular layers and a 55% decrease in the parvocellular layers, and a 30 % decrease of neuron density in the magnocellular and parvocellular layers in the LHON patient. This was associated with extremely severe axonal loss (99%) in the optic nerve (Rizzo et al., 2012).

4.3. Possible role of surviving retinal ganglion cells

The quasi-normal circadian rhythms in some blind individuals (Aubin et al., 2018; Aubin et al., 2016; Aubin et al., 2017) might be partly due to the survival of melanopsin containing intrinsically photosensitive retinal ganglion cells (ipRGCs). The ipRGCs have rudimentary visual functions (Zaidi et al., 2007) and are responsible for residual light perception and visual awareness in some CB. Transgenic CRX-/- mice that lack the outer segment of the photoreceptors have a significantly thinner retinal ganglion cell layer but with intact ipRGCs (Rovsing et al., 2010) and have a normal circadian rhythm. This could explain to some extent the presence of an athrophied optic nerve and its projections to the brain. Indeed, the invasion of the image forming visual system by surviving ipRGC might be one of the factors explaining why the thalamo-cortical pathway survives in blind individuals. Further research on the contribution of melanopsin-containing cells as a compensatory mechanism in blindness is therefore needed. Cross-modal rewiring (tactile or/and auditory projections to the LGN) and feedback projections from the visual cortex to the LGN provide another mechanism (Kupers and Ptito, 2014b).

5. Study limitations

The manual segmentation of the optic chiasm, nerve and tract may have introduced some bias. However, all segmentations were verified by two independent judges (SP and FT) and whenever there was a disagreement, the segmentations were redone until both observers agreed upon the final result. Our study was entirely macro-anatomical. Future studies should seek to investigate microstructural changes in white matter to better understand the microanatomy and physiology of visual tracts that have lost white matter substance. Finally, future studies should also aim to include optical coherence tomography of the retina to study the link between the integrity of the retina and athrophic changes in the retinofugal projection areas. This might help explain some of the inter-individual variability that was observed in this study and help inform the future development of visual restoration treatment.

5.1. Future perspectives

Our findings may have implications for future treatment modalities attempting to restore vision in the blind. Retinal stem cell treatment and retinal implants are currently under development (Farnum and Pelled, 2020; Fernandez, 2018; Maeda et al., 2019; Mirochnik and Pezaris, 2019). Whether it is possible to reactivate a structurally atrophied subcortical visual system will be critical for the success of these technologies (reviewed in Ptito et al., 2021). It is possible that these treatment modalities may only benefit a very select proportion of patients with sufficiently preserved visual white matter pathways. It may therefore prove essential to obtain more comprehensive knowledge on patient-related factors that protect against grey and white matter atrophy such as level and character of residual vision, cause, age of onset and duration of blindness, etc. in order to be able predict who is most likely to benefit most from visual restoration treatments.

6. Conclusion

Volumes of the optic nerve, optic chiasm, optic tract and LGN in CB and LB are roughly half of those measures in sighted controls. Onset of blindness (congenital or acquired) had no significant effect. Reduced voxel intensity ratios suggest a reduced myelin content in both CB and LB. We did not find a correlation between measures of atrophy and blindness duration index in the LB group. Future studies should therefore include subjects who lost vision more recently. Potential consequences of the observed atrophy on the efficacy of treatment modalities seeking to restore vision in the blind remain to be investigated.

Declaration of Competing Interest

The authors declare that they have no known competing financial interests or personal relationships that could have appeared to influence the work reported in this paper.

Acknowledgements

The study was supported by grants from the Lundbeck foundation (Denmark) and the Harland Sanders Foundation (Montreal). The authors would like to thank Nina Reislev for collecting the MRI data of the Copenhagen cohort, Frederik Fiederspiel and Sune Darkner (University of Copenhagen) for their contribution to an early version of this work, and also the volunteers who have participated in the study.

References

Abbott, C.W., Kozanian, O.O., Huffman, K.J., 2015. The effects of lifelong blindness on murine neuroanatomy and gene expression. Front. Aging Neurosci. 7, 144.
Andrews, T.J., Halpern, S.D., Purves, D., 1997. Correlated size variations in human visual cortex, lateral geniculate nucleus, and optic tract. J. Neurosci. 17, 2859–2868.
Aubin, S., Christensen, J.A., Jennum, P., Nielsen, T., Kupers, R., Ptito, M., 2018. Preserved sleep microstructure in blind individuals. Sleep Med. 42, 21–30.
Aubin, S., Gacon, C., Jennum, P., Ptito, M., Kupers, R., 2016. Altered sleep–wake patterns in blindness: a combined actigraphy and psychometric study. Sleep Med. 24, 100–108.
Aubin, S., Kupers, R., Ptito, M., Jennum, P., 2017. Melatonin and cortisol profiles in the absence of light perception. Behav. Brain Res. 317, 515–521.
Beatty, R.M., Sadun, A.A., Smith, L.E.H., Vonsattel, J.P., Richardson, E.P., 1982. Direct demonstration of transsynaptic degeneration in the human visual system: a comparison of retrograde and anterograde changes. J. Neurol. Neurosurg. Psychiatry 45, 143–146.
Bedny, M., Pascual-Leone, A., Dodell-Feder, D., Fedorenko, E., Saxe, R., 2011. Language processing in the occipital cortex of congenitally blind adults. Proc. Natl. Acad. Sci. 108, 4429–4434.

Bottomley, P.A., Hart Jr, H.R., Edelstein, W.A., Schenck, J.F., Smith, L.S., Leue, W.M., Mueller, O.M., Redington, R.W., 1984. Anatomy and metabolism of the normal human brain studied by magnetic resonance at 1.5 Tesla. Radiology 150, 441–446.
Breitenseher, M., Uhl, F., Wimberger, D.P., Deecke, L., Trattnig, S., Kramer, J., 1998. Morphological dissociation between visual pathways and cortex: MRI of visually-deprived patients with congenital peripheral blindness. Neuroradiology 40, 424–427.
Bridge, H., Jindahra, P., Barbur, J., Plant, G.T., 2011. Imaging reveals optic tract degeneration in hemianopia. Invest. Ophthalmol. Vis. Sci. 52, 382–388.
Burgel, U., Amunts, K., Hoemke, L., Mohlberg, H., Gilsbach, J.M., Zilles, K., 2006. White matter fiber tracts of the human brain: threedimensional mapping at microscopic resolution, topography and intersubject variability. NeuroImage 29, 1092–1105.
Butt, O.H., Benson, N.C., Datta, R., Aguirre, G.K., 2013. The fine-scale functional correlation of striate cortex in sighted and blind people. J. Neurosci. 33, 16209–16219.
Cavaliere, C., Aiello, M., Soddu, A., Laureys, S., Reislev, N.L., Ptito, M., Kupers, R., 2020. Organization of the commissural fiber system in congenital and late-onset blindness. Neuroimage Clin. 25, 102133 https://doi.org/10.1016/j.nicl.2019.102133.
Cecchetti, L., Ricciardi, E., Handjaras, G., Kupers, R., Ptito, M., Pietrini, P., 2016. Congenital blindness affects diencephalic but not mesencephalic structures in the human brain. Brain Struct. Funct. 221, 1465–1480.
Chabot, N., Charbonneau, V., Laramée, M.-E., Tremblay, R., Boire, D., Bronchti, G., 2008. Subcortical auditory input to the primary visual cortex in anophthalmic mice. Neurosci. Lett. 433, 129–134.
Charbonneau, V., Laramée, M.-E., Boucher, V., Bronchti, G., Boire, D., 2012. Cortical and subcortical projections to primary visual cortex in anophthalmic, enucleated and sighted mice. Eur. J. Neurosci. 36, 2949–2963.
Desgent, S., Ptito, M., 2012. Cortical GABAergic interneurons in cross-modal plasticity following early blindness. Neural Plast. 2012, 590725 https://doi.org/10.1155/2012/590725.
Eickhoff, S.B., Stephan, K.E., Mohlberg, H., Grefkes, C., Fink, G.R., Amunts, K., Zilles, K., 2005. A. new SPM toolbox for combining probabilistic cytoarchitectonic maps and functional imaging data. NeuroImage 25, 1325–1335.
Farnum, A., Pelled, G., 2020. New Vision for Visual Prostheses. Front. Neurosci. 14 https://doi.org/10.3389/fnins.2020.00036.
Fernandez, E., 2018. Development of visual Neuroprostheses: trends and challenges. Bioelectron. Med. 4, 12.
Fortin, M., Voss, P., Lord, C., Lassonde, M., Pruessner, J., Saint-Amour, D., Rainville, C., Lepore, F., 2008. Wayfinding in the blind: larger hippocampal volume and supranormal spatial navigation. Brain 131, 2995–3005.
Frezzotti, P., Giorgio, A., Motolese, I., De Leucio, A., Iester, M., Motolese, E., Federico, A., De Stefano, N., 2014. Structural and functional brain changes beyond visual system in patients with advanced glaucoma. PLoS One 9, e105931.
Gupta, N., Greenberg, G., De Tilly, L.N., Gray, B., Polemidiotis, M., Yücel, Y.H., 2009. Atrophy of the lateral geniculate nucleus in human glaucoma detected by magnetic resonance imaging. Br. J. Ophthalmol. 93, 56–60.
Hagiwara, A., Hori, M., Kamagata, K., Warntjes, M., Matsuyoshi, D., Nakazawa, M., Ueda, R., Andica, C., Koshino, S., Maekawa, T., 2018. Myelin measurement: Comparison between simultaneous tissue relaxometry, magnetization transfer saturation index, and T 1 w/T 2 w ratio methods. Sci. Rep. 8, 1–12.
Heine, L., Bahri, M.A., Cavaliere, C., Soddu, A., Laureys, S., Ptito, M., 2015. Prevalence of increases in functional connectivity in visual, somatosensory and language areas in congenital blindness. Front. Neuroanat. 9, 86.
Hernowo, A.T., Boucard, C.C., Jansonius, N.M., Hooymans, J.M., Cornelissen, F.W., 2011. Automated morphometry of the visual pathway in primary open-angle glaucoma. Invest Ophthalmol Vis Sci 52, 2758–2766.
Hickey, T.L., Guillery, R.W., 1979. Variability of laminar patterns in the human lateral geniculate nucleus. J. Comp. Neurol. 183, 221–246.
Hoffmann, M.B., Dumoulin, S.O., 2015. Congenital visual pathway abnormalities: a window onto cortical stability and plasticity. Trends Neurosci. 38, 55–65.
Jiang, J., Zhu, W., Shi, F., Liu, Y., Li, J., Qin, W., Li, K., Yu, C., Jiang, T., 2009. Thick visual cortex in the early blind. J. Neurosci. 29, 2205–2211.
Karlen, S.J., Kahn, D.M., Krubitzer, L., 2006. Early blindness results in abnormal corticocortical and thalamocortical connections. Neuroscience 142, 843–858.
Kelly, K.R., McKetton, L., Schneider, K.A., Gallie, B.L., Steeves, J.K., 2013. Altered anterior visual system development following early monocular enucleation. Neuroimage Clinical 4, 72–81.
Kelter, R., 2020. Bayesian alternatives to null hypothesis significance testing in biomedical research: a non-technical introduction to Bayesian inference with JASP. BMC Med. Res. Methodol. 20, 1–12.
Keysers, C., Gazzola, V., Wagenmakers, E.-J., 2020. Using Bayes factor hypothesis testing in neuroscience to establish evidence of absence. Nat. Neurosci. 23 (7), 788–799.
Kosior-Jarecka, E., Pankowska, A., Polit, P., Stępniewski, A., Symms, M.R., Kozioł, P., Żarnowski, T., Pietura, R., 2020. Volume of lateral geniculate nucleus in patients with glaucoma in 7Tesla MRI. J. Clin. Med. 9, 2382.
Kozanian, O.O., Abbott, C.W., Huffman, K.J., 2015. Rapid changes in cortical and subcortical brain regions after early bilateral enucleation in the mouse. PLoS One 10, e0140391. https://doi.org/10.1371/journal.pone.0140391.
Krug, K., 2012. Principles of function in the visual system. In: Sensory Perception. Springer, pp. 41–56.
Kupers, R., Ptito, M., 2014a. Structural, metabolic and functional changes in the congenitally blind brain. Int. J. Psychophysiol. 2, 152.
Kupers, R., Ptito, M., 2014b. Compensatory plasticity and cross-modal reorganization following early visual deprivation. Neurosci. Biobehav. Rev. 41, 36–52.
Lee, J.Y., Jeong, H.J., Lee, J.H., Kim, Y.J., Kim, E.Y., Kim, Y.Y., Ryu, T., Cho, Z.-H., Kim, Y.-B., 2014. An investigation of lateral geniculate nucleus volume in patients with primary open-angle glaucoma using 7 tesla magnetic resonance imaging. Invest. Ophthalmol. Vis. Sci. 55, 3468–3476.
Lee, M.D., Wagenmakers, E.-J., 2014. Bayesian Cognitive Modeling: A Practical Course. Cambridge University Press.
Liu, Y., Yu, C., Liang, M., Li, J., Tian, L., Zhou, Y., Qin, W., Li, K., Jiang, T., 2007. Whole brain functional connectivity in the early blind. Brain 130, 2085–2096.
Maeda, A., Mandai, M., Takahashi, M., 2019. Gene and induced pluripotent stem cell therapy for retinal diseases. Annu. Rev. Genomics Hum. Genet. 20, 201–216.
Manara, R., Citton, V., Maffei, P., Marshall, J.D., Naggert, J.K., Milan, G., Vettor, R., Baglione, A., Vitale, A., Briani, C., 2015. Degeneration and plasticity of the optic pathway in Alström syndrome. Am. J. Neuroradiol. 36, 160–165.
Mcketton, L., Kelly, K.R., Schneider, K.A., 2014. Abnormal lateral geniculate nucleus and optic chiasm in human albinism. J. Comp. Neurol. 522, 2680–2687.
Meaidi, A., Jennum, P., Ptito, M., Kupers, R., 2014. The sensory construction of dreams and nightmare frequency in congenitally blind and late blind individuals. Sleep Med. 15, 586–595.
Mirochnik, R.M., Pezaris, J.S., 2019. Contemporary approaches to visual prostheses. Mil. Med. Res. 6, 19. https://doi.org/10.1186/s40779-019-0206-9.
Müller, F., Niso, G., Samiee, S., Ptito, M., Baillet, S., Kupers, R., 2019. A thalamocortical pathway for fast rerouting of tactile information to occipital cortex in congenital blindness. Nat. Commun. 10, 1–9.
Noppeney, U., 2007. The effects of visual deprivation on functional and structural organization of the human brain. Neurosci. Biobehav. Rev. 31, 1169–1180.
Ogawa, S., Takemura, H., Horiguchi, H., Terao, M., Haji, T., Pestilli, F., Yeatman, J.D., Tsuneoka, H., Wandell, B.A., Masuda, Y., 2014. White matter consequences of retinal receptor and ganglion cell damage. Invest. Ophthalmol. Vis. Sci. 55, 6976–6986.
Pan, W.-J., Wu, G., Li, C.-X., Lin, F., Sun, J., Lei, H., 2007. Progressive atrophy in the optic pathway and visual cortex of early blind Chinese adults: a voxel-based morphometry magnetic resonance imaging study. Neuroimage 37, 212–220.
Papadopoulou, A., Gaetano, L., Pfister, A., Altermatt, A., Tsagkas, C., Morency, F., Brandt, A.U., Hardmeier, M., Chakravarty, M.M., Descoteaux, M., 2019. Damage of the lateral geniculate nucleus in MS: Assessing the missing node of the visual pathway. Neurology 92, e2240–e2249.
Ptito, M., Bleau, M., Djerourou, I., Paré, S., Schneider, F.C., Chebat, D.-R., 2021. Brain-machine interfaces to assist the blind. Front. Hum. Neurosci. 15, 46.
Ptito, M., Schneider, F.C., Paulson, O.B., Kupers, R., 2008. Alterations of the visual pathways in congenital blindness. Exp. Brain Res. 187, 41–49.
Reislev, Kupers, R., Siebner, H.R., Ptito, M., Dyrby, T.B., 2016a. Blindness alters the microstructure of the ventral but not the dorsal visual stream. Brain Struct. Funct. 221, 2891–2903.
Reislev, N.H., Dyrby, T.B., Siebner, H.R., Lundell, H., Ptito, M., Kupers, R., 2017. Thalamocortical connectivity and microstructural changes in congenital and late blindness. Neural Plast. 2017, 9807512. https://doi.org/10.1155/2017/9807512.
Reislev, N.H., Dyrby, T.B., Siebner, H.R., Kupers, R., Ptito, M., 2016b. Simultaneous assessment of white matter changes in microstructure and connectedness in the blind brain. Neural Plast. 2016, 6029241. https://doi.org/10.1155/2016/6029241.
Rizzo, G., Tozer, K.R., Tonon, C., Manners, D., Testa, C., Malucelli, E., Valentino, M.L., La Morgia, C., Barboni, P., Randhawa, R.S., 2012. Secondary post-geniculate involvement in Leber's hereditary optic neuropathy. PLoS One 7, e50230.
Rovsing, L., Rath, M.F., Lund-Andersen, C., Klein, D.C., Møller, M., 2010. A neuroanatomical and physiological study of the non-image forming visual system of the cone-rod homeobox gene (Crx) knock out mouse. Brain Res. 1343, 54–65.
Schmidt, M.A., Knott, M., Heidemann, R., Michelson, G., Kober, T., Dörfler, A., Engelhorn, T., 2018. Investigation of lateral geniculate nucleus volume and diffusion tensor imaging in patients with normal tension glaucoma using 7 tesla magnetic resonance imaging. PLoS One 13, e0198830.
Schmitz, B., Schaefer, T., Krick, C.M., Reith, W., Backens, M., Käsmann-Kellner, B., 2003. Configuration of the optic chiasm in humans with albinism as revealed by magnetic resonance imaging. Invest. Ophthalmol. Vis. Sci. 44, 16–21.
Shimony, J.S., Burton, H., Epstein, A.A., McLaren, D.G., Sun, S.W., Snyder, A.Z., 2006. Diffusion tensor imaging reveals white matter reorganization in early blind humans. Cereb. Cortex 16, 1653–1661.
Tomaiuolo, F., Campana, S., Collins, D.L., Fonov, V.S., Ricciardi, E., Sartori, G., Pietrini, P., Kupers, R., Ptito, M., 2014. Morphometric changes of the corpus callosum in congenital blindness. PLoS One 9, e107871.
Tomaiuolo, F., Di Paola, M., Caravale, B., Vicari, S., Petrides, M., Caltagirone, C., 2002. Morphology and morphometry of the corpus callosum in Williams syndrome: a T1-weighted MRI study. Neuroreport 13, 2281–2284.
Wang, D., Qin, W., Liu, Y., Zhang, Y., Jiang, T., Yu, C., 2013. Altered white matter integrity in the congenital and late blind people. Neural Plast. 2013, 128236 https://doi.org/10.1155/2013/128236.
Watkins, K.E., Shakespeare, T.J., O'Donoghue, M.C., Alexander, I., Ragge, N., Cowey, A., Bridge, H., 2013. Early auditory processing in area V5/MT+ of the congenitally blind brain. J. Neurosci. 33, 18242–18246.
You, Y., Gupta, V.K., Graham, S.L., Klistorner, A., 2012. Anterograde degeneration along the visual pathway after optic nerve injury. PLoS One 7, e52061.
Zaidi, F.H., Hull, J.T., Peirson, S.N., Wulff, K., Aeschbach, D., Gooley, J.J., Brainard, G. C., Gregory-Evans, K., Rizzo III, J.F., Czeisler, C.A., 2007. Short-wavelength light sensitivity of circadian, pupillary, and visual awareness in humans lacking an outer retina. Curr. Biol. 17, 2122–2128.